

IEEE 1984 Ultrasonics Symposium Proceedings

IEEE Press, New York, 1984

TRANSIENT RADIATION FROM FOCUSED TRANSDUCERS

Daniel Guyomar and John Powers
 Department of Electrical and Computer Engineering
 Naval Postgraduate School
 Monterey, California 93943

Abstract

A method based on the time extension of the angular spectrum theory of diffraction is presented for computing the transient field radiated from a curved surface (or a plane surface having either a time-delay excitation or, equivalently, an acoustic lens in front of it). Such field descriptions are of interest in acoustical imaging and scattering. The model gives a linear systems oriented interpretation of the focusing process. It can be applied for arbitrary transducer geometries or for arbitrary acoustic lens profiles (or time-delays), providing a useful tool for transducer design. The method uses FFT routines for time-efficient computer evaluation. The ability to use arbitrary time sampling intervals allows flexible inspection of the diffraction pattern. For radially symmetric sources the technique allows rapid determination of the wave boundary locations without requiring the computation of the field. Computer simulations of sources, including spherical focused, parabolic focus and conical focus sources are included.

Introduction

Calculation of the field from pulsed focused ultrasonic transducers has become important in recent years [1-7] due to the emphasis on pulsed medical imaging systems. This paper describes a technique for the efficient computer computation of the transient field of a curved wave front. This wave front can be produced from a focused transducer, from a planar array with proper phasing to produce the curved wave, or from a wave that has transited an acoustic lens. It is assumed that the curved wave passes through an aperture in a rigid baffle and that the medium is linear, homogeneous, and lossless. The wave curvature is limited to avoid reflections of the wave from the opposite side of the transducer. The technique is based on the spatial impulse technique used by Stepanishen [8-10] for the solution of fields from planar sources in baffles, but uses a spatial frequency domain interpretation of the solution to give a physical explanation of the propagation as the application of a time-varying spatial filter. The method is applied to focused concave, conical and parabolic waves as examples of its application.

Basic theory

For a planar rigid-baffled transducer, it is known from diffraction theory that the velocity potential is related to the source velocity distribution by

$$\phi(x, y, z, t) = \tau(t) s(x, y) \ast \ast \ast [\delta(ct-R)/R] \quad (1)$$

where $s(x, y)$ and $\tau(t)$ represent the space and time-varying parts of the known velocity disturbance at the input plane and $\ast \ast \ast$ indicates convolution performed over the indicated variable. The expression $\delta(ct-R)/R$ in Eq. 1 is the Green's function for free space propagation.

The curvature of the wave can be modelled by a spatially variable delay $d(x, y)$ from a plane wave. For a separable velocity disturbance the field can be written as

$$\phi(x, y, z, t) = \gamma(t) \ast \ast \ast_t s(x, y) \delta[ct-d(x, y)] \ast \ast \ast \frac{\delta(ct-R)}{R} \quad (2)$$

where $d(x, y)$ is the spatial offset of the curved wave front from a plane wave. All one needs for the propagation technique to be described is a description of the wave front in terms of either its relative displacement, $d(x, y)$, or its time delay, $\Delta(x, y)$.

Because of the difficulty of the spatial convolutions in Eq. 2, it is convenient to use the spatial frequency domain. Propagation in this domain corresponds to a time generalization of the angular spectrum theory, leading to a linear systems interpretation of the transient diffraction. A key transform in the development (for an radially symmetric source) is

$$B[\delta(ct-R)/R] = J_0[\rho(c^2 t^2 - z^2)^{1/2}] H(ct-z) \quad (3)$$

where $B[\cdot]$ is the Hankel transform operator, and $\rho = (f_x^2 + f_y^2)^{1/2}$. Assuming axial symmetry, the transform of the potential due to a temporal impulse of the form, $\delta[ct-d(x)]$, can be written from Eqs. 2 and 3 as

$$H(f_x, f_y, z, t) = B[s(x)\delta[ct-d(x)] \ast \ast \ast_t J_0[\rho(c^2 t^2 - z^2)^{1/2}] H(ct-z) \quad (4)$$

The transform on the right side of Eq. 4 can be evaluated [11] as

$$B[s(r)\delta(ct-d(r))] = \sum_{i=1}^N \frac{s(r_i^*) J_0(\rho r_i^*) r_i^*}{\left| \frac{\partial d(r)}{\partial r} \right|_{r=r_i^*}} \cdot \frac{J_0[\rho(c^2 t^2 - z^2)^{1/2}]}{t} \quad (5)$$

where $r_i^*(y)$ represents the values of r for which $d(r)-ct=0$. Here, N is the number of r_i^* . (Appendix A displays expressions for the relative displacement $d(r)$, the r_i^* , and the derivative in the denominator of Eq. 5 for various wave front configurations.)

The temporal impulse response $h(x,y,z,t)$ is obtained by inverse transforming Eq. 5 to give

$$h(x,y,z,t) = B^{-1} \left[\sum_{i=1}^N \frac{s(r_i^*) J_0(\rho r_i^*) r_i^*}{\left| \frac{\partial d(r)}{\partial r} \right|_{r=r_i^*}} \cdot \frac{J_0[\rho(c^2 t^2 - z^2)^{1/2}]}{t} \right] \quad (6)$$

This equation gives the output field for an axially symmetric surface velocity when excited by an impulse in time. The curvature of the field is contained in the expressions for r_i^* . (Reference 11 contains equations that are valid for all cases, not just the axisymmetric.)

The terms of the summation represent the angular spectrum of a circular line source weighted by the function, $s(r_i^*)$. The radius of such a line varies with time according to the delay law since r_i^* is a function of time. The resulting field is just the summation of these line-generated waves plus the diffraction field that has been generated by the previous line excitations. The field computation requires only one convolution for the computed frequencies and a Hankel transform.

Again, solutions for an arbitrary time excitation may be obtained by convolution of the impulse response with the time excitation as in Eq. 2.

Numerical Simulations

Once the geometry of the transducer is known, an elementary calculation leads to the relative displacement of the wave, $d(r)$. Then the N zeros of $ct-d(r)$ are calculated. These are $r_i^*(y)$. These solutions are then used in Eq.6. Standard algorithms perform the transforms. The convolution is done numerically for each spatial frequency. The results of the convolution are then inverse transformed to give the resulting values of the field. (It is worth noting that the calculation of the convolution uses the same products required for the transform, thereby reducing the computational complexity of the required operations.)

If the displacement, $d(r)$, is a monotonic function, then the intersection with the plane, $z=ct$, will reduce to a closed line and the summa-

tion in the equations will reduce to a single term. This is usually the case for a focused wave.

The following simulations have been investigated using this technique: circular wave fronts with concave curvatures of spherical, conical and paraboloid shapes. The corresponding delays for each of these shapes is given in Appendix A.

The computations were done on a grid of 64x64 spatial sample points and 50 time samples. The plots show one spatial dimension vs. time for a median through the center of the transducer. The complete three-dimensional calculation consumes approximately 80 seconds of CPU computer time on an IBM 3033 mainframe computer. For convenience the plots have been normalized to a maximum value of one. The time axis as well as the width axis are expressed in terms of one characteristic size, A , of the transducer (either half-width or radius, as appropriate). The time axis has a zero value at the time when the first wave reaches the observation line. The focal length f is 10 cm in all cases. The transducer radius, A , is assumed to be 2.0 cm and the excitation is an impulse (except for Fig. 6).

Figures 1-3 show the diffraction pattern from a circular wave front with a spherical concave surface. The receiving plane is located at distances of $f/2$, f , and $2f$ from the front edge of the source. While the solution of Eq. 6 is obtained in a plane parallel to the excited surface the plots have been shown with time as the variable to allow comparison with existing solutions [2,3]. The results fit the closed form solution of Refs. 2 and 3 very well. Symmetry is observed when the field is observed at the focal distance (Fig. 2).

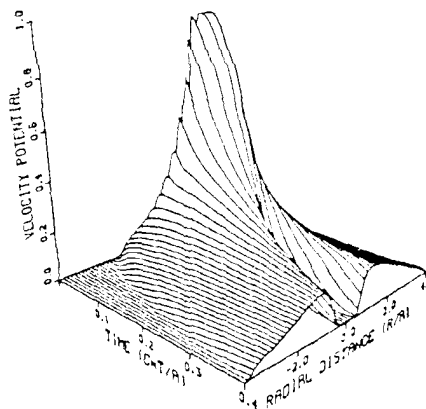


Figure 1 Spherical concave wave with a circular cross-section (Impulse excitation, $A=2.0$ cm, $f= 10$ cm, $z=5$ cm)

Figures 4 and 5 represent focussed wave fronts with a conical and parabolic concave surface at the focal plane.

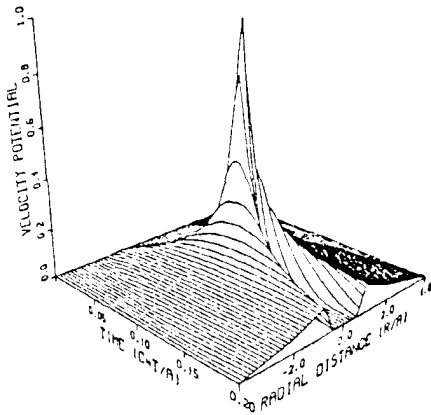


Figure 2 Spherical concave wave with a circular cross-section (Impulse excitation, $A=2.0$ cm, $f=10$ cm, $z=10$ cm)

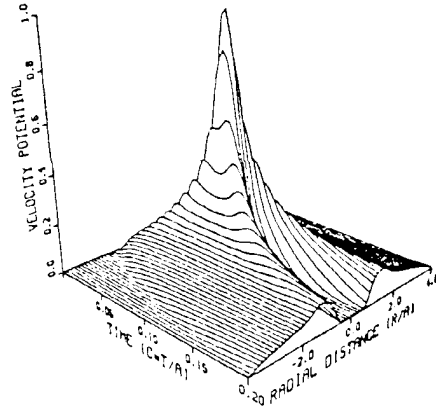


Figure 4 Conical concave wave with a circular cross-section (Impulse excitation, $A=2.0$ cm, $f=10$ cm, $z=10$ cm)

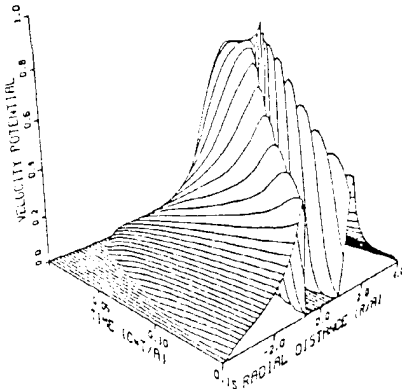


Figure 3 Spherical concave wave with a circular cross-section (Impulse excitation, $A=2.0$ cm, $f=10$ cm, $z=20$ cm)

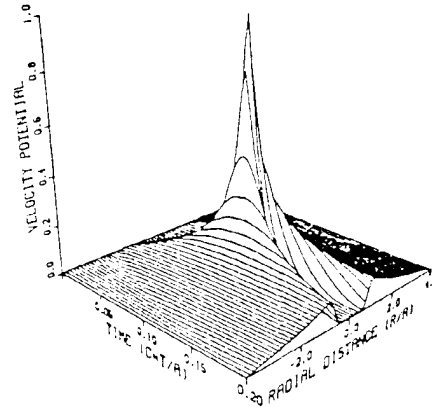


Figure 5 Parabolic concave wave with a circular cross-section (Impulse excitation, $A=2.0$ cm, $f=10$ cm, $z=10$ cm)

For a time excitation different than $\delta(t)$, the diffracted wave is a convolution between the impulse response and the excitation function. Figure 6 shows the result of a spherical concave pattern observed at the focal point. The excitation is a positive rectangular pulse with a duration of $0.04A/c$, where A is lateral half-width of the input wave front. The smoothing effect of the time domain convolution is evident along the propagation axis.

Summary

A general approach for computing the radiated field of axial symmetry has been developed. Equation 6 gives an expression for the impulse response of the field. In most practical applications the expressions leading to the field simplify as can be seen in Appendix A, providing a useful tool for transducer design. The method does not re-

quire any specific sample interval in the time domain allowing a variable sampling interval as warranted. Once the impulse-excited response is known, it can be stored and the transient response for arbitrary time excitations can be computed by performing the time domain convolution. A 50 point convolution for all of the 64 spatial data points requires 1.4 s on an IBM 3033 computer.

Acknowledgements

This work was partially supported by the Foundation Research Program of the Naval Postgraduate School. Daniel Guyomar is a Research Associate of the National Research Council.

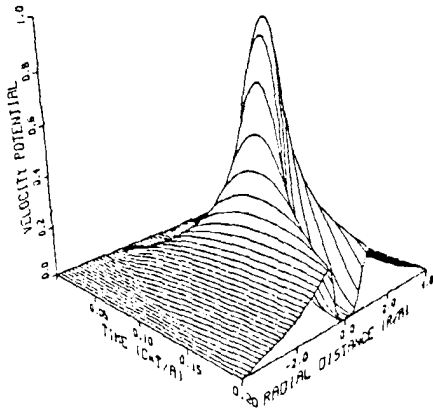


Figure 6 Spherical concave wave with a circular cross-section (Pulse excitation, $T=0.40A/c$, $A=2.0$ cm, $f=10$ cm, $z=10$ cm)

Appendix A

This Appendix gives the relative displacement, $d(r)$, of the curved wave front, the zeros of $ct-d(r)$, and expressions for the derivative of $d(r)$ with respect to r , evaluated at the zeros. All of the relative displacements are given for the same depth, d , given by

$$d = f - (f^2 - a^2)^{1/2} \tag{A1}$$

where a is the depth of a concave lens focusing at a distance, f .

Spherical concave wave front

$$d(r) = (f^2 - r^2)^{1/2} - (f^2 - a^2)^{1/2} \tag{A2}$$

$$r_i^* = [a^2 - c^2 t^2 - 2ct(f^2 - a^2)^{1/2}]^{1/2} \tag{A3}$$

$$\left. \frac{d'(r)}{dr} \right|_{r=r_i^*} = \frac{[a^2 - c^2 t^2 - 2ct(f^2 - a^2)^{1/2}]^{1/2}}{ct + (f^2 - a^2)^{1/2}} \tag{A4}$$

Conical concave wave front

$$d(r) = \frac{-r[f - (f^2 - a^2)^{1/2}]}{a} + f - (f^2 - a^2)^{1/2} \tag{A5}$$

$$r_i^* = \frac{a[f - (f^2 - a^2)^{1/2} - ct]}{f - (f^2 - a^2)^{1/2}} \tag{A6}$$

$$\left. \frac{d'(r)}{dr} \right|_{r=r_i^*} = \frac{f - (f^2 - a^2)^{1/2}}{a} \tag{A7}$$

Parabolic concave wave front

$$d(r) = - \frac{r^2 [f - (f^2 - a^2)^{1/2}]}{a^2} \tag{A8}$$

$$r_i^* = \left[\frac{f - (f^2 - a^2)^{1/2} - ct}{f - (f^2 - a^2)^{1/2}} \right]^{1/2} \tag{A9}$$

$$\left. \frac{d'(r)}{dr} \right|_{r=r_i^*} = \frac{(2/a) [(f - (f^2 - a^2)^{1/2})(f - (f^2 - a^2)^{1/2} - ct)]^{1/2}}{(2/a) [(f - (f^2 - a^2)^{1/2})(f - (f^2 - a^2)^{1/2} - ct)]^{1/2}} \tag{A10}$$

References

1. M. Fink, 'Theoretical study of pulsed echocardiographic focusing procedures', Acoustical Imaging, Vol. 10, P. Alais and A. Metherell, Eds., (Plenum Press, New York, 1980), pp. 437-453
2. A. Penttinen and M. Luukkala, 'The impulse response and pressure nearfield of a curved ultrasonic radiator', J. Phys. D Appl. Phys., 9, pp. 1547-1557, 1976
3. M. Arditi et al., 'Transient fields of concave annular arrays', Ultrasonic Imaging, 3, pp. 37-61, 1981
4. D.R. Dietz, 'Apodized conical focusing for ultrasonic imaging', IEEE Trans. on Son. and Ultrasonics, SU29(3), pp. 128-138, 1982
5. M.M. Goodsitt et al., 'Field patterns of pulsed, focused ultrasonic radiators in attenuating and nonattenuating media', J. Acous. Soc. Am., 71(2), pp. 318-330, 1982
6. W.N. Cobb, 'Frequency domain method for the prediction of ultrasonic field patterns of pulsed, focused radiators', J. Acoust. Soc. Am., 75(1), pp. 72-80, 1984
7. M.S. Patterson and F.S. Foster, 'Acoustic field of conical radiators', IEEE Trans. on Son. and Ultrasonics, SU29(2), pp. 83-91, 1982
8. P.R. Stepanishen, 'Transient radiation from pistons in an infinite planar baffle', J. Acoust. Soc. Am., 49(5), pp. 1629-1637, 1971
9. P.R. Stepanishen, 'Experimental verification of the impulse response method to evaluate transient acoustic fields', J. Acoust. Soc. Am. 63(6), pp. 1610-1617, 1981
10. G.R. Harris, 'Review of transient field theory for a baffled planar piston', J. Acoust. Soc. Am., 70(1), pp. 10-20, 1981
11. D. Guyomar and J. Powers, 'Transient fields radiated by curved surfaces- application to focusing', To be published in J. Acoust. Soc. Am.